ENGINEERING TRANSACTIONS • *Engng. Trans.* • **59**, 3, 235–248, 2011
Polish Academy of Sciences • Institute of Fundamental Technological Research (IPPT PAN)
National Engineering School of Metz (ENIM)

DYNAMIC COMPRESSION TESTS – CURRENT ACHIEVEMENTS AND FUTURE DEVELOPMENT

W. M o ć k o [1)], Z.L. K o w a l e w s k i [1,2)]

[1)] **Institute of Fundamental Technological Research**
Polish Academy of Sciences
Pawińskiego 5B, 02-106 Warszawa, Poland
e-mail: wmocko@ippt.gov.pl

[2)] **Motor Transport Institute**
Jagiellońska 80, 03-301 Warszawa, Poland

In this paper a modified arrangement of the DICT technique was introduced. Miniaturization of bar and use of shadow principle to make a measurement of displacement allow to obtain strain rate up to 2.2×10^5 s^{-1}. Commonly used methods of elimination of friction, inertia and adiabatic heating were presented. In order to estimate the rate sensitivity of a material (tantalum), quasi-static and SPHB tests were performed at room temperature within the rate spectrum ranging from 5×10^{-4} s^{-1} to 10^3 s^{-1}. The final true stress versus true strain curves at different strain rates were corrected to a constant temperature and zero friction.

Key words: direct impact compression tests, tantalum, Hopkinson bars, miniaturized arrangement.

1. Introduction

It is known for a long time that most materials are dependent on the rate of deformation and temperature. At strain rates above $\sim 10^3$ s^{-1} the strain rate sensitivity for most metals and alloys substantially increases and an accurate and complete picture is necessary in formulation of constitutive relations in the range of the strain rate spectrum up to $\sim 10^6$ s^{-1}.

Although advances in electronics and recordings of short time processes have caused that compression impact experiments are much easier to perform at present, still some improvements in both mechanical designs and measuring techniques are possible. One possibility, which is more recently observed, is miniaturization of experimental setups. The miniaturization enables not only for a substantial increase of strain rate but also for reduction of the radial and longitudinal inertia of specimen. The miniaturization concept has been employed in this study in order to reach strain rates up to $\sim 10^5$ s^{-1}.

One of the most popular experimental techniques applied in determination of viscoplastic properties of materials at strain rates from $\sim 5 \times 10^2$ s^{-1} to $\sim 10^4$ s^{-1} is the Kolsky apparatus [1] or the so-called Split Hopkinson Pressure Bar (SHPB). A modified version of the Kolsky apparatus, the version that is used in most laboratories up to now, has been developed by LINDHOLM [2]. In both versions, a wafer specimen is placed between bars. Such an experimental technique can be applied in many configurations, for example in compression [3, 4], tension [5, 6], torsion [7, 8] and in shear [9, 10], and also in different sizes. In the case of compression test, the wafer specimens are prone to friction and inertia. Moreover, the use of the SHPB technique is limited by the elastic limit of the incident bar. According to the one-dimensional elastic wave propagation theory the "safe" maximum impact velocity is directly related to the elastic limit of the incident bar [1]. Such a condition limits the maximum strain rate in the test.

In order to reach strain rates higher than $\sim 10^4$ s^{-1}, DHARAN and HAUSER [11] introduced modification of the SHPB concept by elimination of the incident bar. Thus, application of the direct impact of a striker onto wafer specimen supported by the transmitter bar enabled to reach strain rates $\sim 10^5$ s^{-1}. Such a modification can be defined as the Direct Impact Compression Test (DICT). It is clear that elimination of the incident bar and reduction of the specimen size leads to a substantial increase of the maximum nominal strain rate in DICT experimental technique. The maximum strain rate $\sim 10^5$ s^{-1} attained by further miniaturization of the DICT up to 1.5 mm transmitter bar diameter was also reported in literature [12].

Of course, specimen reduction can be applied for both SHPB and DICT arrangements. A specimen reduction must be performed proportionally to the length-to-diameter ratio l_{S0}/d_{S0}, usually ~ 0.5 because of optimization of friction and inertia effects [3, 13, 14]. As a consequence of the specimen reduction the whole arrangement, that is SHPB or DICT, must be also reduced. Several attempts to reduce the SHPB size, that is the striker and both bars, were reported in the past [12, 15, 16]. Another miniaturization of SHPB has been reported in 1992 by SAFFORD [17]. The wave dispersion was taken into account. In general, for elastic bars of small dimensions the wave dispersion is a second order effect. A new design and some problems associated with miniaturization were published more recently [18]. Those examples indicate that miniaturization of the conventional SHPB arrangement enables to reach the maximum strain rate $\sim 4.5 \times 10^4$ s^{-1}.

In both cases, namely the conventional and miniaturized DICT arrangements, the technical problem arises how to determine the displacement of the interface striker-specimen as a function of time. This technical problem has been solved in several ways:

- assuming that the striker is perfectly rigid [11],
- applying of a high-speed camera incorporating an optical system with the image-splitting refraction element and lens [16, 19],
- using a two-channel non-contact displacement gage [20, 21],
- following radial displacement of the specimen shadow [22], the so-called LORD (Laser Occlusive Radius Detector).

2. Miniaturized DICT arrangement

A new miniaturized DICT is shown schematically in Fig. 1 [23, 24]. Modification in the mechanical part, similar as reported earlier [25], lies in an introduction of the decelerator tube *5* in to which a small Hopkinson bar *3* with miniature SR gages *4* is inserted. The decelerator tube is mounted in supports *7* slightly ahead of the a Hopkinson bar *3* with a possibility to change the distance between them. Such configuration permits programming of different plastic deformations of specimens. The tube and the bar are both attached to the bumper *8*. The tube can be exactly adjusted to the axis of striker *2* by special support *6*, which also prevents vibrations. In Fig. 2 are shown the main details of the miniaturized DICT. The striker (No. *2* in Fig. 1) of diameter slightly lower than that of the decelerator tube (No. *5* in Fig. 1) triggers deformation of a small cylindrical specimen until it stops by the decelerator tube. The transmitted elastic wave is detected by the SR gage (No. *4* in Fig. 1). The net displacement between the striker and the decelerator tube is measured by the shadow technique. Strikers of diameter 11 mm and of different lengths from 12.5 mm to 50 mm can be launched by an air-gun up to 100 m/s. Specimens of diameter 2.0 mm and lengths from 1.0 mm to 0.8 mm were supported by the transmitter bar of

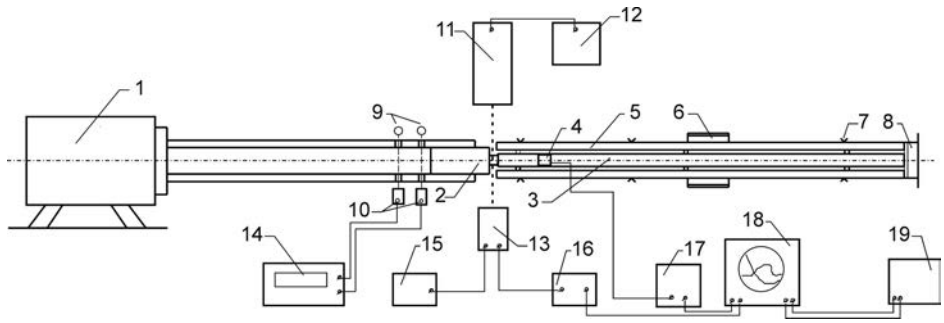

Fig. 1. General scheme of DICT, *1* – air gun; *2* – striker; *3* – transmitter bar; *4* – SR gage; *5* – decelerator tube; *6* – main support; *7* – supports; *8* – dumper; *9* – light sources; *10* – photodiodes; *11* – laser diode; *12* – supply of *11*; *13* – photodiode (displacement measurement); *14* – time counter; *15* – supply unit of *13*; *16* – DC amplifier; *17* – SR amplifier; *18* – digital oscilloscope; *19* – PC.

diameter 5.2 mm and length 243 mm. The transmitter bar was made of the maraging steel with the yield stress of 2.1 GPa. The relative distance between the tube and the transmitter bar could be varied from 0 up to 2.0 mm. This distance defines the maximum deformation of the specimen. In addition, in the application of the combination tube – the bar enables to recover specimens after testing, thus giving an opportunity to observe some microstructural effects. The arrangement permits also for tests with a negative jump in strain rate [25, 26].

The scheme of measurements is shown schematically in Fig. 1. Three independent circuits permit for precise measurement of the impact velocity V_0, the net displacement during specimen deformation $\Delta U(t) = \Delta l_S(t)$, and the transmitted elastic wave $\varepsilon_T(t)$, where t is time.

The striker is accelerated in the launcher tube *1* of length 840 mm up to preprogrammed impact velocity after pressure calibration, that is $V_0(p)$. The mean impact velocity V_0 is determined by two channels consisting of two laser diodes *9*, two diaphragms of diameter 0.5 mm and two photodiodes *10*. The axes of the laser diodes and photodiodes perpendicular to the direction of the launcher tube are situated at 140 mm and 60 mm from the specimen, respectively. Thus, the distance over which the impact velocity is measured is 80 mm. Signals from the photodiodes are recorded by the time counter.

The net displacement, and thus the net mean velocity V_{AV} of specimen deformation, is measured by the principle of shadow, Fig. 1 and Fig. 2, and the wave mechanics in the Hopkinson bar. The light emitted by laser diode *11* is formed by a diaphragm and goes through the gap in between the moving striker and the stationary deceleration tube. During the test the gap is closing up when the specimen is deformed. The displacement of the interface striker/specimen is proportional to the light passed by the gap. The transmitted light is detected by photodiode *13*, the photodiode is supplied by the unit *15*. The electric signal from the photodiode after amplification in *16* is recorded by two-channel digital oscilloscope *18*. It is clear that after calibration the photodiode voltage can be transformed into the displacement of the interface striker/specimen versus time.

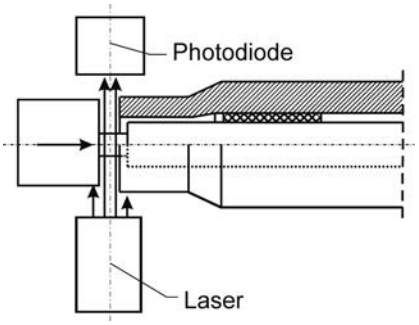

FIG. 2. Zoom of the specimen arrangement.

The displacement of the specimen/transmitter bar can be determined via recording of the signal from the two SR gages of length 0.6 mm cemented on the opposite sides of the transmitter bar. The signals from the SR gages are recorded by the second channel of digital oscilloscope *18* next, the records of both channels are transmitted into PC, No. *19* in Fig. 1.

The definition of the nominal strain rate is given by:

$$\dot{\varepsilon}_n(t) = \frac{1}{l_{S0}} \left[\frac{dU_A(t)}{dt} - \frac{dU_B(t)}{dt} \right]. \tag{2.1}$$

Introducing into Eq. (2.1) the quantities recorded by the DICT measurement system leads to:

$$\dot{\varepsilon}_n(t) = \frac{1}{l_{S0}} \left[\frac{dU_A(t)}{dt} - C_0 \varepsilon_T(t) \right], \tag{2.2}$$

where $U_A(t)$ – displacement of the striker/specimen interface, C_0 – elastic wave speed in transmitter bar, $\varepsilon_T(t)$ – transmitted elastic wave.

The nominal strain $\varepsilon_n(t)$ can be found by integration of Eq. (2.2), thus

$$\varepsilon_n(t) = \frac{1}{l_{S0}} \left[U_A(t) - C_0 \int \varepsilon_T(t)\, dt \right], \qquad 0 < t < T. \tag{2.3}$$

If strikers are assumed being rigid during the whole process of specimen deformation, and their kinetic energies are sufficiently high, then deceleration of a striker is zero. The rigid striker was assumed by Dharan and Hauser [11] in the first version of the DICT. However, in a more exact analysis it may be assumed that deceleration of the interface A is proportional to time, then $a_A = -Bt$, where B is a constant determined from the test via $U_A(t)$ record. This procedure assures flexibility and eliminates difficulties in finding $V_A(t)$ by the time derivative of $U_A(t)$. If $B = 0$, then the deceleration is constant. In general case the velocity $V_A(t)$ is given by

$$V_A(t) = V_0 - B \int_0^t \xi d\xi \qquad \text{and} \qquad V_A(t) = V_0 - \frac{1}{2} B t^2, \qquad 0 < t < T. \tag{2.4}$$

From Eqs. (2.1) and (2.2) one obtains the nominal quantities $\dot{\varepsilon}_n(t)$ and $\varepsilon_n(t)$. The parameters in Eq. (2.4): V_0, B and T must be determined from experiment. Approximation of Eq. (2.4) leads to the following formulas:

$$\dot{\varepsilon}_n(t) = \frac{1}{l_{S0}} \left[V_0 - \left[B \int_0^t \xi d\xi + C_0 \varepsilon_T(t) \right] \right]. \tag{2.5}$$

After integration, the nominal strain is given by:

$$\varepsilon_n(t) = \frac{1}{l_{S0}} \left[V_0 t - \left[\frac{B}{2} t^2 + C_0 \int_0^t \varepsilon_T(\xi) d\xi \right] \right]. \tag{2.6}$$

Of course, the true strain $\varepsilon(t)$ can be obtained from the standard formula $\varepsilon(t) = ln(1 - \varepsilon_n(t))$.

The nominal stress, $\sigma_n(t) \approx F_B(t)/A_{S0}$, in the specimen can be obtained as a function of time assuming that the force equilibrium occurs during the entire process of specimen deformation. This assumption, which is a good approximation for very short specimens, should be in general confirmed every time, for example by a FE analysis. In the present case the specimen is very short, $l_{S0} = 0.8$ mm, and the transit time of the elastic wave through the specimen is $\Delta t_S = 160$ ns. It is well recognized that after 3 to 5 transits the force equilibrium is satisfied [27]. In the present case, $3\Delta t_S = 480$ ns and this period of time is much shorter than the total time of deformation $T = 20$ μs at strain rate 2×10^4 s^{-1}. In real tests the total time of deformation is still longer. The force F_B in the transmitter bar is determined after introduction of Hooke's law:

$$F_B(t) = A_b \rho C_0^2 \varepsilon_T(t), \tag{2.7}$$

where A_b is the cross-section area of the transmitter bar. Thus, the average nominal stress σ_n is given by:

$$\sigma_n(t) = \rho_S C_0^2 \left(\frac{d_H}{d_{S0}} \right)^2 \varepsilon_T(t), \tag{2.8}$$

where d_{S0} and d_H are respectively the initial diameter of specimen and diameter of the transmitter bar, $d_H > d_{S0}$, ρ_S is the density of the specimen material. Because all constitutive relations are defined in true values, that is true stress, true strain and true strain rate, it is important to transform the nominal values into the true quantities like $\sigma(t)$, $\varepsilon(t)$ and $\dot{\varepsilon}(t)$. After elimination of time, the final material characterization can be found: $\sigma(\varepsilon)$ and $\dot{\varepsilon}(\varepsilon)$.

3. Elimination of friction, inertia and adiabatic heating

It is well known that friction occurring on the specimen interfaces with platens during quasi-static compression test increases the mean axial pressure [13, 14, 27, 28]. By integration of the equation of force equilibrium several authors estimated in the past the effect of friction at different levels of approximation. For example, Siebel [28] derived an approximate formula for the mean stress on the cylindrical specimen in terms of the axial yield stress;

$$\overline{\sigma} = \sigma\left(1 + \frac{4\mu d_{S0}}{3l_{S0}}\right) \qquad \text{or} \qquad \sigma = \overline{\sigma}\left(1 + \frac{4\mu d_{S0}}{3l_{S0}}\right)^{-1}, \tag{3.1}$$

where $\overline{\sigma}$ and σ are respectively the mean stress determined from experiment and the net flow stress of a material, μ is the coefficient of Coulomb friction and d_{S0} is the initial specimen diameter. If the coefficient of friction is known then the flow stress of a material can be found. For example, for specimen dimensions $l_{S0} = 1.0$ mm, $d_{S0} = 2.0$ mm and $\mu = 0.06$ the relative increment of stress is $(\overline{\sigma}/\sigma) - 1 = 0.04$, the increase is only 4.0%. It is interesting to note that the coefficient of dynamic friction is lower as a rule than the quasi-static one (slow gliding) [29].

Another possibility to reduce the friction effects is application of a ring specimen [30]. Application of ring specimens in dynamic tests was also reported in several papers [11, 16, 31]. In conclusion, the effect of friction in determination of the flow stress in fast compression tests with a good lubrication is expected to be relatively limited in comparison to other effects like the radial and longitudinal specimen inertia.

Effects of inertia in DICT are very important because of high accelerations and mass velocities observed in such circumstances. One possibility of estimating the radial inertia is integration of the equation of the quantity of movement in the radial direction and application of the Huber-Mises yield condition [11, 20, 32], then

$$\sigma(t) = \overline{\sigma}(t) - \frac{3}{8}\rho\left(\frac{2d_{S0}}{l_{S0}}\right)^2 \frac{V^2(t)}{(1 - \varepsilon_S(t))^2}, \tag{3.2}$$

where $V(t)$ is the current axial velocity of specimen compression $V(t) = V_A(t) - V_B(t)$. The second term in Eq. (3.2) is the stress correction for the radial inertia.

The early numerical analysis of both friction and inertia in SHPB was reported in 1975 [27]. Nowadays many numerical analyses have been published on specimen behavior in high-speed compression and it is out of scope of this paper to review those results.

The most general solutions for both effects, the friction and inertia in the form of overstress, is given by [13, 33]:

$$\Delta\sigma = \frac{\mu\overline{\sigma}}{3s} + \frac{\rho d_S^2}{12}\left(s^2 - \frac{3}{16}\right)(\dot{\varepsilon}_1^2 + \ddot{\varepsilon}) + \frac{3\rho d_S^2}{64}\ddot{\varepsilon}, \tag{3.3}$$

where s is the current ratio of the specimen length to the specimen diameter, $s = l_S/d_S$. The effect of the convection velocity is not taken into consideration. The first term appears because of friction and the next two are the results of inertia. The second term vanishes for all specimens satisfying the conditions:

$s^2 - 3/16 = 0$, or when $\dot{\varepsilon}^2 + \ddot{\varepsilon} = 0$ which may occur for $t > t_r$, where t_r is the rise time of the initial portion of the transmitted wave $\varepsilon_T(t)$. The ratio $s_D = \sqrt{3}/4$, ($s_D = 0.433$) for Poisson's ratio $\nu = 1/2$ was derived as the optimal one by DAVIES and HUNTER [3], but under assumption $\mu = 0$. According to Eq. (3.3) the stress difference $\Delta\sigma = \overline{\sigma} - \sigma$ shows the absolute minimum and the following s_{opt} is determined as:

$$s_{\text{opt}} = \left[\frac{2\mu\overline{\sigma}}{\rho d_S^2(\dot{\varepsilon}^2 + \ddot{\varepsilon})}\right]^{1/3}. \tag{3.4}$$

One of the most important problems in correct determination of stress-strain characteristics at high and very high strain rates is the thermal softening of specimen material caused by adiabatic heating. The adiabatic heating caused by conversion of plastic work into thermal energy triggers an auto-coherent process of the material softening leading to a decrease of the tangent modulus of stress-strain curve and consequently to a decrease of the flow stress when plastic deformation increases. Because of a positive strain rate sensitivity the process intensifies at very high strain rates. In the final stages of compression some forms of mechanical instability appear in the form of Adiabatic Shear Bands (ASB) leading to failure [34–36]. Since at lower strain rates, typically $\dot{\varepsilon} < 10\ \text{s}^{-1}$, plastic deformation is practically isothermal, in order to make comparison the adiabatic stress-strain characteristics obtained at higher strain rates than $\sim 10^2\ \text{s}^{-1}$ should be corrected into isothermal conditions [34]. A simple correction procedure that was applied in this paper was given earlier [34].

The stress correction for the adiabatic increase of temperature used in further analysis of DICT experiments reported in this paper is given by:

$$\Delta\sigma(\varepsilon)_{\dot{\varepsilon}} \approx \frac{\vartheta\beta\sigma_o f(\dot{\varepsilon})\varepsilon}{\rho(T_0)C_p(T_0)} \qquad \text{or} \qquad \Delta\sigma(\varepsilon)_{\dot{\varepsilon}} \approx A\sigma_o\varepsilon f(\dot{\varepsilon}). \tag{3.5}$$

It can be shown that this approximation is relatively exact for mild steels because of a very limited strain hardening at high strain rates [34]. Of course, the highest decrease of stress caused by adiabatic heating occurs for large plastic strains, when the mean stress and the temperature sensitivity are high and the density and the specific heat are low. Since $f(\dot{\varepsilon})$ is an increasing function of strain rate the effect of adiabatic heating intensifies at high strain rates.

In conclusion, the correction of the flow stress from adiabatic to isothermal conditions becomes more important at high and very high strain rates. After correction into isothermal conditions the constitutive surface $(\sigma, \varepsilon, \dot{\varepsilon})_{T_0} = 0$ can be determined for any metallic material.

4. Experimental results

Compression tests of the polycrystalline tantalum were performed at room temperature in as-received state at five strain rates: 10^{-4} s^{-1}, 10^{-2} s^{-1}, 2.6×10^3 s^{-1}, 2.6×10^3 s^{-1}, 1.1×10^5 s^{-1}, 2.2×10^5 s^{-1}. The tests at static deformation regime were performed on servo-controlled universal machine. The diameter of specimens was $d_{S0} = 5.14$ mm and initial length was $l_{S0} = 2.5$ mm, what gave the initial aspect ratio $s_0 = 0.5$. In order to minimize friction effects a lubrication of MoS2 was applied.

Dynamic compression tests of tantalum at high rates of deformation were carried out at one strain rate of 2.6×10^3 s^{-1} with the use of SHPB of diameter $d_H = 20$ mm with application of the two-wave analysis, which consists of incident and transmitted waves. Dynamic compression tests at very high rates of deformation were performed applying miniaturized DICT method at two strain rates of 1.1×10^5 s^{-1} and 2.2×10^5 s^{-1}. The stress-strain curve has been corrected for adiabatic heating, Eq. (3.5). Thus, all curves were transformed into the isothermal conditions. It is noted that tantalum shows substantial strain rate sensitivity. The final set of quasi-static and dynamic $\sigma(\varepsilon)$ curves is shown in Fig. 3. The range of strain rate is nine decimal orders, that is from 10^{-4} s^{-1} to 2.2×10^5 s^{-1}. All curves are in true coordinates and corrected to isothermal conditions. The effect of strain rate on the flow stress is shown in Fig. 4 for three levels of strain. The rate sensitivity $\beta = (\partial\sigma/\partial \log \dot{\varepsilon})_\varepsilon$ shows two ranges, at lower strains $\beta \approx 46$ MPa and $\beta \approx 260$ MPa above the strain rate threshold $\dot{\varepsilon}_C \approx 1000$ s^{-1}.

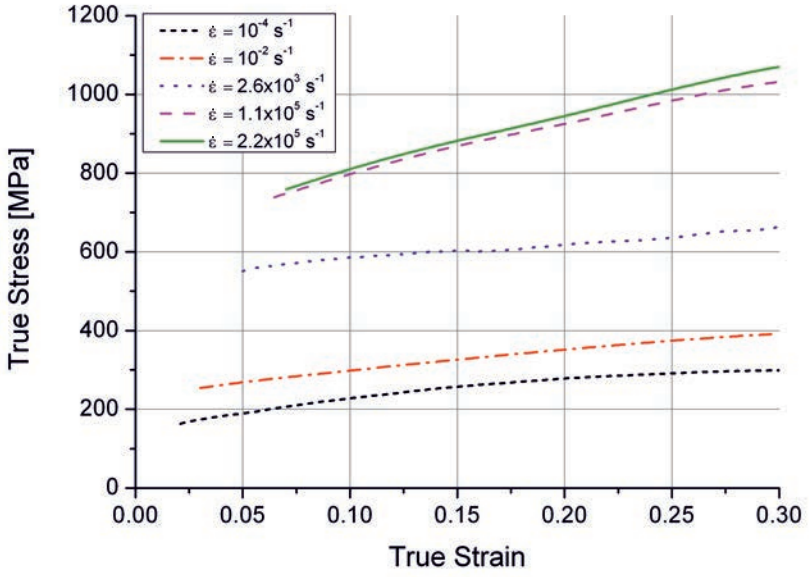

Fig. 3. True stress vs. true strain curves of tantalum at different strain rates.

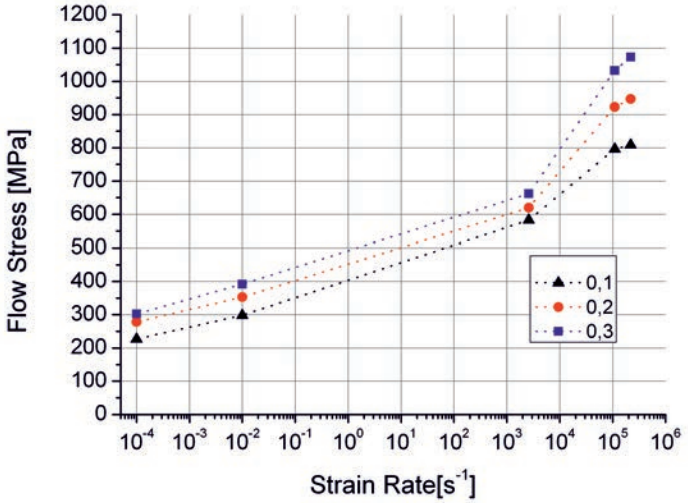

FIG. 4. Rate sensitivity of tantalum at three levels of true strain.

Such, a result suggests existence of two thermally activated dislocation micromechanisms of plastic deformation in those two ranges of strain rate [34].

Figure 5 shows optical micrographs of the as-received tantalum. Grains are regular without any deformations. Grain boundaries are straight at particular sections. Optical micrograph of the material after deformation at rate of 10^{-4} s^{-1} is shown in Fig. 6. Grains are strongly deformed in direction of the applied force. Grain boundaries are irregular and curved. Moreover, the shear bands along two main directions of shearing may be observed in particular grains. Hollows coming from etching shows that a large number of dislocations has occurred which is in agreement with the knowledge concerning plastic deformation mechanisms. Similar effects could be observed for tantalum after prestrain at strain rate of 5×10^3 s^{-1} (Fig. 7).

a) b)

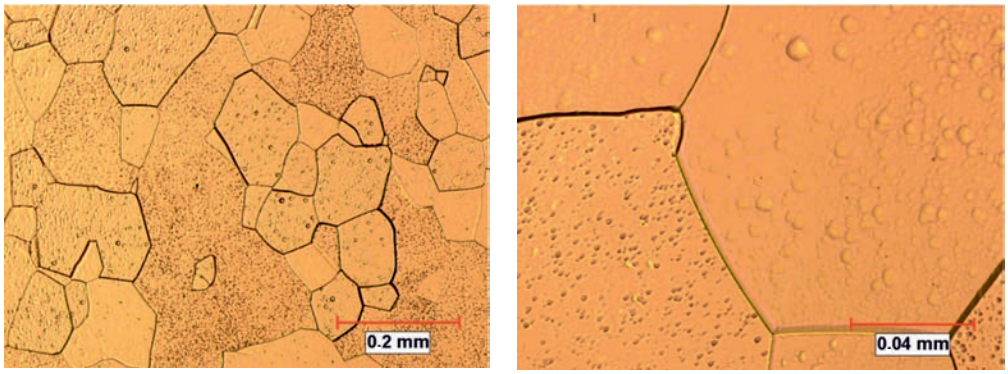

FIG. 5. Optical micrograph of the as-received tantalum at various magnifications.

a) b)

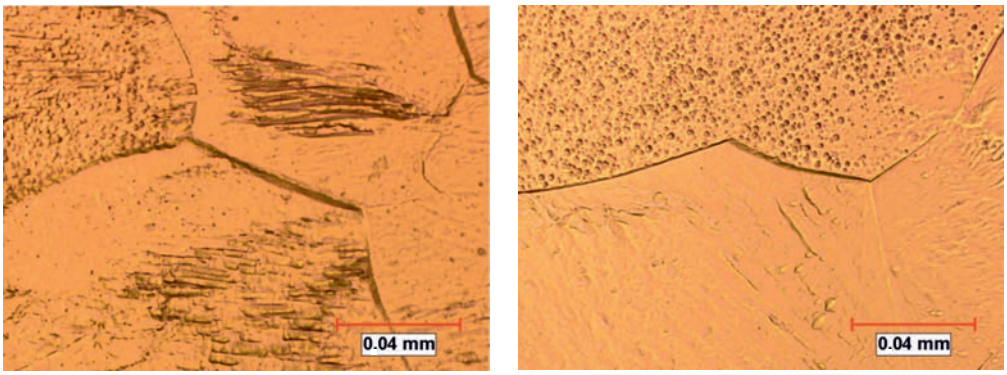

FIG. 6. Optical micrograph of tantalum prestrained using strain rate of 10^{-4} s^{-1}, a) longitudinal cross-section, b) transverse cross-section.

a) b)

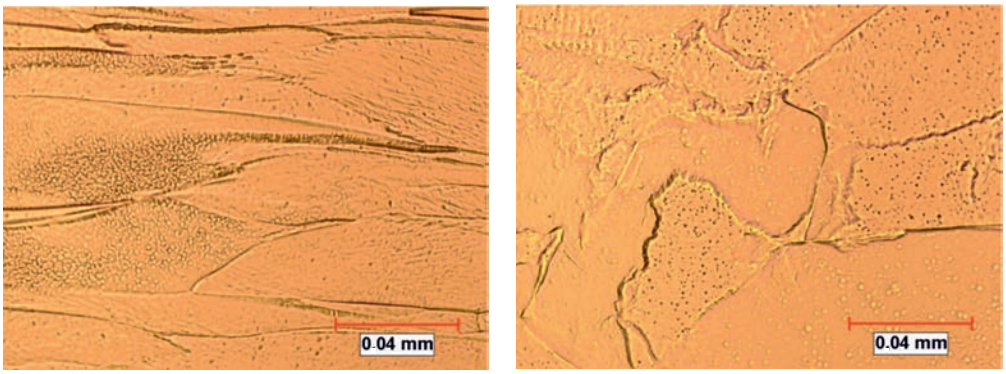

FIG. 7. Optical micrograph of tantalum prestrained using strain rate of 5×10^3 s^{-1}, a) longitudinal cross-section, b) transverse cross-section.

5. Discussion and conclusions

Introduction of specimen miniaturization in high strain rate materials testing, in both cases of SHPB and DICT, enables reaching of high strain rates up to $\sim 10^5$ s^{-1}. Typical dimensions applied in miniaturized tests are 1.0 mm $< l_{S0} <$ 2.0 mm, 1.0 mm $< d_{S0} <$ 2.0 mm and $0.5 < s_0 < 1.0$. Such specimen dimensions reduce substantially the effects of inertia reducing at the same time errors when the inertia analysis is neglected. Although a simple inertia analysis or even FE calculations are recommended, application of very small specimens assures minimum errors in determination of material behavior at very high strain rates. Previous analyses of the inertia effects related to the specimen dimensions indicated that the stress increment due to inertia raises

rapidly with strain rate and with specimen dimensions [37]. The strain rate threshold from the thermally activated rate sensitivity to the so-called pseudo-viscosity [9, 11] must be carefully evaluated in the future. On the other hand, specimen miniaturization leads to limitation of grain number in small specimens. For example, if the specimen volume is $v_s = 6.28$ mm^3 ($d_{S0} = 2.0$ mm and $l_{S0} = 0.5$ mm) and the mean grain diameter is 0.1 mm then the volume of each grain is $v_{gr} = 3.15 \times 10^{-3}$ mm^3 and the number of grains in the specimen volume is $N \approx 2 \times 10^3$. Probably this value is a minimum representative for measurement of the mean behavior.

Application of small diameter Hopkinson bars substantially reduces dispersion of elastic waves. Because in DICT technique strain gages are cemented closely to the specimen-bar interface, recommended distance $\sim 5\ d_H$, where d_H is diameter of Hopkinson bar, the transmitted wave gives not much distorted signal from the interface. In addition, the bar vibration in the longitudinal mode superimposed on the transmitted wave is relatively low [3]. However on the other hand it is impossible to monitor the force equilibrium, that is $F_A(t)$ and $F_B(t)$ as a function of time, and the force equilibrium must be assumed. One possibility is an analytic estimation or application a FE code. Because specimens applied in the miniaturized DICT are short the stress gradients within a typical specimen are assumed to be small.

In the version of the DICT arrangement reported in this paper the original and not expensive optical technique to measure displacement of the interface striker-specimen has been applied. Therefore, combination of the opto-electronic measurement of the displacement of interface A and theory of elastic wave propagation enabling measurement of the displacement of interface B, has provided an exact measurement of the specimen strain and strain rate as a functions of time.

Combination of the quasi-static precision compression test, along with application of SHPB along with the miniaturized DICT, makes possible determination of the rate sensitivity of materials for very wide strain rate spectrum, from 10^{-4} s^{-1} to 2.2×10^5 s^{-1}.

References

1. H. Kolsky, *An Investigation of the Mechanical Properties of Materials at Very High Rates of Loading*, Proc. Phys. Soc. London, **62B**, 676, 1949.

2. U. S. Lindholm, *Some Experiments with the Split Hopkinson Pressure Bar*, J. Mech. Phys. Solids, **12**, 5, 317, 1964.

3. E. D. H. Davies, S. C. Hunter, *The Dynamic Compression Testing of Solids by the Method of the Split Hopkins Pressure Bar*, J. Mech. Phys. Solids, **11**, 155, 1963.

4. U. S. Lindholm, L. M. Yeakley, *Dynamic Deformation of Single and Polycrystalline Aluminium*, J. Mech. Phys. Solids, **13**, 41, 1965.

5. J. Harding, E. O. Wood, J. D. Cambell, *Tensile Testing of Materials at Impact Rates of Strain*, J. Mech. Eng. Sci., **2**, 88, 1960.

6. T. Nicholas, *Tensile Testing of Materials at High Rates of Strain, Experimental Mechanics*, **21**, 177, 1981.

7. J. Duffy, J. D. Campbell, R. M. Hawley, *On the Use of a Torsional Split Hopkinson Bar to Study Rate Effects in 1100-0 Aluminium*, J. Appl. Mech., **93**, 3, 83, 1971.

8. P. E. Sensey, J. Duffy, R. M. Hawley, *Experiments on Strain Rate History and Temperature Effects During the Plastic Deformation of Close-Packed Metals*, J. Appl. Mech., Trans. ASME, **45**, 60, 1978.

9. J. D. Campbell, W. G. Ferguson, *The Temperature and Strain-Rate Dependence of the Shear Strength of Mild Steel*, Phil. Mag., **81**, 63, 1970.

10. J. Harding, J. Huddart, *The Use of the Double-Notch Shear Test in Determining the Mechanical Properties of Uranium at Very High Rates of Strain*, Proc. Conf. On Mech. Prop. at High Rates of Strain, Oxford, Conf. Ser., **47**, 49, 1979.

11. C. K. M. Dharan, F. E. Hauser, *Determination of Stress – Strain Characteristic at Very High Strain Rates, Experimental Mechanics*, **10**, 370, 1970.

12. F. Kamler, P. Niessen, R. J. Pick, *Measurement of the Behavior of High Purity Copper at Very High Rates of Strain*, Canad. J. Phys., **73**, 295, 1995.

13. J. Z. Malinowski, J. R. Klepaczko, *A Unified Analytic and Numerical Approach to Specimen Behaviour in the SHPB*, Int. J. Mech. Sci., **28**, 381, 1986.

14. D. A. Gorham, P. H. Pope, O. Cox, *Sources of Error in Very High Strain Rate Compression Tests*, Proc. Conf. on Mech. Prop. at High Rates of Strain, Oxford, Conf. Ser., **70**, 151, 1984.

15. U. S. Lindholm, *Deformation Maps in the Region of High Dislocation Velocity*, Proc. IUTAM Symposium on High velocity Deformation of Solids, Tokyo, 1977, Springer-Verlag, Berlin Haidelberg New York, **26**, 1978.

16. D. A. Gorham, *Measurement of Stress-Strain Properties of Strong Metals at Very High Rates of Strain*, Proc. Conf. On Mech. Prop. At High Rates Strain, Oxford, Conf. Ser., **47**, 16, 1979.

17. N. A. Safford, *Materials Testing up to 10^5 s^{-1} Using a Miniaturized Hopkinson Bar with Dispersion Corrections*, Proc. 2nd Int. Symp. on Intense Dynamic Loading and its Efects, Sichuan University Press, Chengdu, China, 378, 1992.

18. D. Jia, K. T. Ramesh, *A Rigorous Assessment of the Benefits of Miniaturization in the Kolsky Bar System*, Experimental Mechanics, **44**, 445, 2004.

19. D. A. Gorham, *A Numerical Method for the Correction of Dispersion in Pressure Bar Signals*, J. Phys. E: Sci. Instrum., **16**, 477, 1983.

20. J. R. Klepaczko, *Advanced Experimental Techniques in Materials Testing*, [in:] *New Experimental Methods in Material Dynamics and Impact*, IPPT, Polish Academy of Sciences, Warsaw, p. 223, 2002.

21. D. Ostwald, J. R. Klepaczko, P. Klimanek, *Compression Tests of Polycrystalline α-Iron up to High Strains Over a Large Range of Strain Rates*, J. Phys. IV, Colloque C3, France, **7**, C3/385, 1997.

22. K. T. Ramesh, S. Narasimhan, *Finite Deformations and the Dynamic Measurement of Radial Strains in Compression Kolsky Bar Experiments*, Int. J. Solids Structures, **33**, 3723, 1996.

23. J. Z. Malinowski, J. R. Klepaczko, Z. L. Kowalewski, *Miniaturized compression test at very high strain rates by direct impact*, Experimental Mechanics, **47**, 451–463, 2007.

24. J. M. Malinowski, J. R. Klepaczko, Z. L. Kowalewski, *Modified version of the direct impact compression test technique*, Dynamic Behaviour of Materials – J.R. Klepaczko Workshop, Metz, 13–15 maj 2009.

25. J. Shioiri, K. Sakino, S. Santoh, *Strain Rate Sensitivity of Flow Stress at Very High Rates of Strain*, IUTAM Symp. Constitutive Relation in High/Very High Strain Rates, Kawata K. and Shioiri J. [Eds.], Springer-Verlag, Tokyo, **49**, 1966.

26. K. Sakino, J. Shioiri, *Dynamic Flow Stress Response of Aluminum to Sudden Reduction in Strain Rate at Very High Strain Rates*, J. Phys. IV, Colloque C3, France, **1**, C3/35, 1991.

27. L. D. Bertholf, C. H Karnes, *Two Dimensional Analysis of the Split Hopkinson Pressure Bar System*, J. Mech. Phys. Solids, **23**, 1, 1975.

28. E. Siebel, *Grundlagen zur Berechnung des Kraft und Arbeitbedorf bei Schmieden und Walzen*, Stahl und Eisen, **43**, 1295, 1923.

29. R. S. Montgomery, *Friction and Wear at High Sliding Speeds*, Wear, **36**, 275, 1976.

30. B. Avitzur, *Forging of Hollow Discs*, Israel Journal of Technology, **2**, 3, 295, 1964.

31. M. Ashton, D. J. Perry, *A Constitutive Relationship for Metals Compensated for Adiabatic and Friction Effects*, Proc. 6th Int. Conf. on Mechanical and Physical Behaviour of Materials under Dynamic Loading, Kraków, 263, 2000.

32. J. R. Klepaczko, F. E. Hauser, *Radial Inertia in Compression Testing of Materials*, Technical Report (internal), Division of Inorganic Materials, University of California, Berkeley, 1969.

33. J. Z. Malinowski, *Cylindrical Specimen Compression Analysis in the Split Hopkinson Pressure Bar System*, Engng. Trans., **35**, 4, 551, 1987.

34. J. R. Klepaczko, J. Duffy, *Strain Rate History Effects in Body-Center-Cubic Metals*, ASTM-STP 765, 251, 1982.

35. J. R. Klepaczko, *Generalized Conditions for Stability in Tension Test*, Int. J. Mech. Sci., **10**, 297, 1968.

36. S. L. Semiatin, J. J. Jonas, *Formability and Workability of Metals*, ASM, Metals Park, Ohio, 1984.

37. D. A. Gorham, *An Effect of Specimen Size in the High Strain Rate Compression Test*, Proc. Conf. Dymat, Coll. C3, suppl. Journal de Physique III, **1**, C3-411, 1991.

Received May 16, 2011; revised version August 24, 2011.